Journal of Biomechanics 46 (2013) 1031–1034

Contents lists available at SciVerse ScienceDirect

Journal of Biomechanics

journal homepage: www.elsevier.com/locate/jbiomech
www.JBiomech.com

Short communication

A thumb carpometacarpal joint coordinate system based on articular surface geometry

Eni Halilaj [a], Michael J. Rainbow [b], Christopher J. Got [c], Douglas C. Moore [c], Joseph J. Crisco [a,c,*]

[a] Center for Biomedical Engineering and School of Engineering, Brown University, Providence, RI 02912, USA
[b] Department of Physical Medicine and Rehabilitation, Harvard Medical School, Cambridge, MA 02138, USA
[c] Department of Orthopaedics, The Warren Alpert Medical School of Brown University and Rhode Island Hospital, Providence, RI 02903, USA

ARTICLE INFO

Article history:
Accepted 6 December 2012

Keywords:
Articular geometry
Thumb CMC
Anatomical coordinate system
Kinematics
Computed tomography
3-dimensional models

ABSTRACT

The thumb carpometacarpal (CMC) joint is a saddle-shaped articulation whose *in vivo* kinematics can be explored more accurately with computed tomography (CT) imaging methods than with previously used skin-based marker systems. These CT-based methods permit a detailed analysis of the morphology of the joint, and thus the prominent saddle geometry can be used to define a coordinate system that is inherently aligned with the primary directions of motion at the joint. The purpose of this study was to develop a CMC joint coordinate systems that is based on the computed principal directions of curvature on the trapezium and the first metacarpal. We evaluated the new coordinate system using bone surface models segmented from the CT scans of 24 healthy subjects. An analysis of sensitivity to the manual selection of articular surfaces resulted in mean orientation differences of $0.7 \pm 0.7^\circ$ and mean location differences of 0.2 ± 0.1 mm. Inter-subject variability, which mostly emanates from anatomical differences, was evaluated with whole bone registration and resulted in mean orientation differences of $3.1 \pm 2.7^\circ$ and mean location differences of 0.9 ± 0.5 mm. The proposed joint coordinate system addresses concerns of repeatability associated with bony landmark identification and provides a robust platform for describing the complex kinematics of the CMC joint.

1. Introduction

Motion of the thumb is greatly influenced by the articular geometry of the thumb carpometacarpal (CMC) joint—a well-defined saddle that facilitates flexion/extension and adduction/abduction, while partly restraining axial rotation (Chèze et al., 2012; Cooney et al., 1981; Hollister et al., 1992; Imaeda et al., 1994; Pieron, 1973). The range of motion at the CMC joint has been reported to be approximately 53° of flexion/extension, 42° of adduction/abduction, and 17° of axial rotation (Cooney et al., 1981), reflecting the fact that flexion/extension and adduction/abduction are the primary physiological motions in this joint. Other studies have also determined that the primary axes of rotation at the CMC joint are closely aligned with its saddle geometry (Hollister et al., 1992; Imaeda et al., 1994).

The International Society of Biomechanics (ISB) has proposed standardized joint coordinate systems (JCS) for various joints in the human body (Wu et al., 2005), based on Grood and Suntay's knee coordinate system (Grood and Suntay, 1983) which consists of two body-fixed axes—one axis embedded in each bone—and a floating axis that is perpendicular to each of the body-fixed axes. In order to minimize cross-talk in kinematic data reporting, the rotational axis with the least physiological motion should be defined as the floating axis of the JCS. In the knee, adduction/abduction is considerably minor when compared to the other two rotations, and therefore is defined as the floating axis (Grood and Suntay, 1983). However, applying an analogous coordinate system to the thumb CMC joint is not optimal because internal/external rotation of the metacarpal is the smallest physiological rotation. Hence, Cheze et al. (2009) proposed a refinement of the ISB-recommended CMC JCS, in which the flexion/extension and the adduction/abduction axes are the body-fixed axes and the internal/external rotation axis is floating. Using an experimental model, they also demonstrated that their recommended sequence reduced cross-talk among the three rotational motions.

Given an optimal Euler sequence (Cheze et al., 2009), the next step towards a more robust CMC JCS is a rigorous definition of the body-fixed flexion/extension and adduction/abduction axes. Since motion at the CMC joint is governed by the saddle geometry of its articular surfaces, previous CMC joint coordinate systems

* Correspondence to: Bioengineering Laboratory, Department of Orthopaedics, The Warren Alpert Medical School of Brown University and Rhode Island Hospital, 1 Hoppin Street, CORO West, Suite 404, Providence, RI 02903, USA.
Tel.: +1 401 444 4231; fax: +1 401 444 4418.
E-mail address: joseph_crisco@brown.edu (J.J. Crisco).

0021-9290/$ - see front matter © 2013 Elsevier Ltd. All rights reserved.
http://dx.doi.org/10.1016/j.jbiomech.2012.12.002

(Cheze et al., 2009; Cooney et al., 1981; Wu et al., 2005) have been based on anatomical landmarks that seek to align the flexion/extension axis with the concavity and the adduction/abduction axis with the convexity of the saddle-shaped joint. Although axes derived from anatomical landmarks may approximate the concavity and the convexity of the articular surfaces at the CMC joint, the subjective process of landmark selection has limitations. The kinematic errors associated with landmark imprecision have created a need for coordinate system definitions that are intrinsically robust (Della Croce et al., 2005). In the CMC joint, computation of the principal directions of curvature directly from the articular topography rather than through approximation, presents an opportunity for improved accuracy and repeatability.

In this communication we present a semi-automated method for generating a thumb CMC joint coordinate system that is based on the computed principal directions of curvature in the articulation and therefore avoids potential limitations associated with manual landmark identification. We supplement our proposed method with sensitivity and inter-subject variability analyses of *in vivo* data from a set of 24 healthy joints.

2. Methods

2.1. 3D bone models

After receiving approval from the Institutional Review Board and obtaining informed consents, the wrists and thumbs on the dominant hands of 24 healthy volunteers (12 males, age 38.7 ± 11.7 yrs and 12 females, age 43.2 ± 15.8 yrs) were imaged in a clinical neutral position with a 16-slice clinical CT scanner (GE LightSpeed 16, General Electric, Milwaukee, WI). Imaging parameters included tube settings of 80 kVp and 80 mA, slice thickness of 0.625 mm, and in-plane resolution of at least 0.4 mm × 0.4 mm. The trapeziae and the first metacarpals were segmented using Mimics v12.11 (Materialise, Leuven, Belgium) and 3-D bone models were exported as meshed surfaces.

2.2. Segment coordinate system (SCS) generation

The trapezial and the metacarpal segment coordinate systems were based on the principal directions of curvature on the articular surfaces of each 3-D bone model. The borders of the articular surfaces were manually selected in Geomagic Studio (Geomagic, Research Triangle Park, NC) by carefully tracing the visible perimeter of the subchondral bone surfaces (Fig. 1a). A monotone fifth order polynomial surface ($f(x,y)$) was fit to each selected articular surface. The local saddle point ($f(a,b)$) was determined by computing the gradient fields (Fig. 1b), finding the critical points, and performing a second partial derivative test:

$$if \begin{vmatrix} f_{xx}(a,b) & f_{xy}(a,b) \\ f_{yx}(a,b) & f_{yy}(a,b) \end{vmatrix} < 0, \text{then } f(\text{a,b}) \text{ is a saddle point.}$$

A fifth order polynomial surface was chosen because it was the lowest order polynomial with a root-mean-squared (RMS) error of less than 0.1 mm, capturing the salient global features of the saddle while avoiding over-fitting, which includes local features that are of little importance to overall joint motion. Principal directions of curvature were computed for the portion of the surface within 3 mm of the saddle point, and their vector averages—$\boldsymbol{i}$ in the direction of minimum curvature and $\boldsymbol{k}$ in the direction of maximum curvature – were computed (Fig. 1c). The 3 mm threshold was chosen because the bounded points captured the saddle geometry and excluded regions of high shape variation at the edges of the articular surfaces.

Following the ISB convention (Wu and Cavanagh, 1995; Wu et al., 2005), the z-axis of the trapezial coordinate system (Z_{TPM}) was defined by $\boldsymbol{i}_{TPM}$, running in a ulnar-to-radial direction, the y-axis (Y_{TPM}) by the cross product of Z_{TPM} and $\boldsymbol{k}_{TPM}$, oriented in a distal-to-proximal direction, and the x-axis (X_{TPM}) by the cross product of Y_{TPM} and Z_{TPM}, running in a dorsal-to-volar direction. Similarly, X_{MC1} in the metacarpal coordinate system was defined by $\boldsymbol{i}_{MC1}$, Y_{MC1} by the cross product of $\boldsymbol{k}_{MC1}$ and X_{MC1}, and Z_{MC1} as the cross product of the X_{MC1} and the Y_{MC1} (Fig. 1c). The saddle point, served as the origin of each segment coordinate system.

2.3. Joint coordinate system (JCS) definition

Based on the axes of rotation of an idealized saddle (Fig. 2), joint flexion/extension is defined as rotation about the trapezial-fixed Z_{TPM} and joint abduction/adduction as rotation about the metacarpal-fixed X_{MC1}; internal/external rotation then corresponds to rotation about the floating axis (Fig. 3). Using the *ZYX* Euler sequence, this configuration minimizes angular cross-talk in the CMC joint (Cheze et al., 2009). Consistent with the ISB guidelines (Wu et al., 2005), the neutral posture is defined as the position where the axes of the two segment coordinate systems are aligned, and translation of the metacarpal with respect to the trapezium is defined as the translation of the MC1 SCS origin with respect to the TPM SCS.

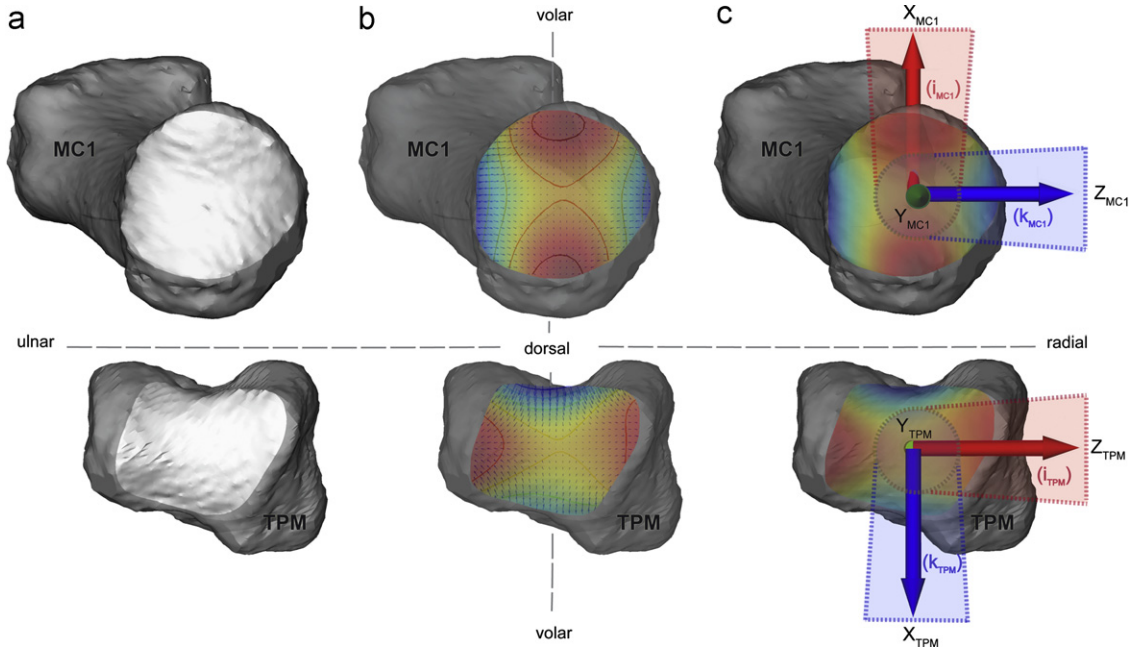

Fig. 1. Exploded views of the trapezium (TPM) and the first metacarpal (MC1) with: (a) the manually-selected subchondral bone surfaces, (b) the 5th order polynomial fits to the articular surfaces, colored by elevation, isocontours of the articular topography, and gradient fields (∇f; at the saddle point, $\nabla f = 0$ and the determinant of the Hessian is less than 0), (c) the trapezial and the metacarpal coordinate systems, where $\boldsymbol{i}$ and $\boldsymbol{k}$ are the average principal direction vectors for points within a 3 mm radius from the saddle point, $Z_{TPM} = \boldsymbol{i}_{TPM}$; $Y_{TPM} = Z_{TPM} \times \boldsymbol{k}_{TPM}$; $X_{TPM} = Y_{TPM} \times Z_{TPM}$; $X_{MC1} = \boldsymbol{i}_{MC1}$; $Y_{MC1} = \boldsymbol{k}_{MC1} \times X_{MC1}$; $Z_{MC1} = X_{MC1} \times Y_{MC1}$.

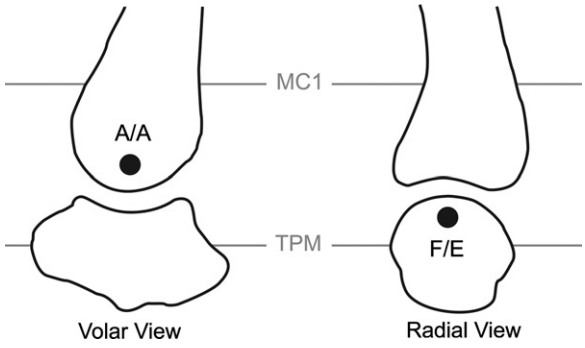

Fig. 2. The joint coordinate system is composed of two body-fixed axes—$\boldsymbol{Z}_{TPM}$ fixed to the trapezium and $\boldsymbol{X}_{MC1}$ fixed to the first metacarpal—and a third, floating, axis that is perpendicular to both of the body-fixed axes. Rotation about $\boldsymbol{Z}_{TPM}$ is defined as extension/flexion, rotation about $\boldsymbol{X}_{MC1}$ is defined as adduction/abduction, and external/internal rotation is defined as rotation about $\boldsymbol{Y}$. **e1**, **e2**, **e3** denote the Euler sequence.

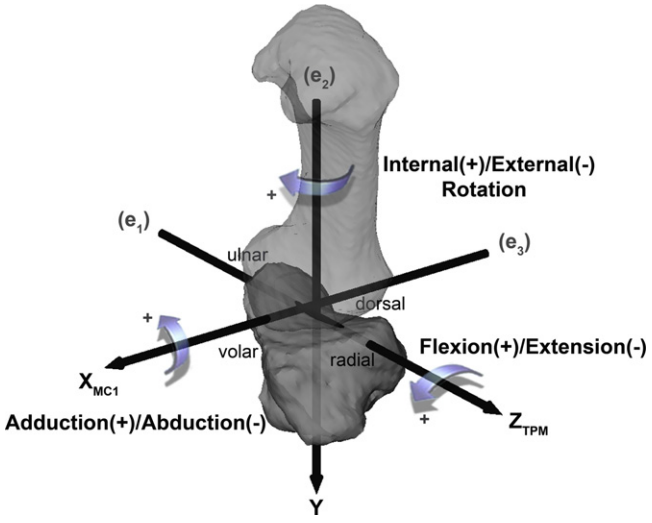

Fig. 3. A simplified schematic representation of the CMC joint as an idealized saddle. Flexion/extension of the first metacarpal (MC1) over the trapezium (TPM) occurs about an axis that pierces the TPM and abduction/adduction occurs about an axis that pierces the MC1. Therefore, the $\boldsymbol{Z}_{TPM}$–$\boldsymbol{Y}$–$\boldsymbol{X}_{MC1}$ sequence was chosen over the $\boldsymbol{X}_{TPM}$–$\boldsymbol{Y}$–$\boldsymbol{Z}_{MC1}$ sequence, or the previously proposed $\boldsymbol{X}_{TPM}$–$\boldsymbol{Z}$–$\boldsymbol{Y}_{MC1}$ sequence.

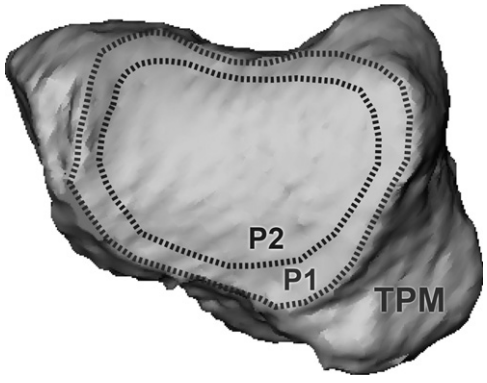

Fig. 4. A distal view of a trapezium, illustrating the optimal surface selection (P_1) and the modified surface selection (P_2).

2.4. SCS sensitivity analysis

The generation of the coordinate systems presented here is mostly automated, with the exception of the articular surface selection. Accordingly, the sensitivity of the orientation and location of the segment coordinate systems to the process of articular surface selection was assessed by re-computing the coordinate systems from surfaces that were selected by following a perimeter (P_2) that was significantly smaller than the visible subchondral perimeter (P_1; Fig. 4). The orientation of their axes and the location of their origins were compared to those of the initially computed coordinate systems. Orientation differences were obtained by computing the dot product of the axes acquired through the differently selected articular surfaces, i.e. given $[XYZ]_{TPM\text{-}P1}$ obtained by following P_1 and $[XYZ]_{TPM\text{-}P2}$ obtained from following P_2, then $\theta_X = \arccos(X_{TPM\text{-}P1} \cdot X_{TPM\text{-}P2})$, $\theta_Y = \arccos(Y_{TPM\text{-}P1} \cdot Y_{TPM\text{-}P2})$, $\theta_Z = \arccos(Z_{TPM\text{-}P1} \cdot Z_{TPM\text{-}P2})$. Location differences were determined by computing the Euclidian distances between the two origins.

2.5. SCS inter-subject variability

To evaluate variability across subjects, trapezial and metacarpal bone models were first isotropically scaled by $\sqrt[3]{V_{avg}}/\sqrt[3]{V_s}$, where V_{avg} is the average bone volume and V_s is the subject specific bone volume. After scaling, all the bones were registered in Geomagic Studio, and the resulting kinematic transforms were applied to the respective coordinate systems. The average x-, y-, and z-axes and the average origins were computed for both the TPM SCS and MC1 SCS. Inter-subject variability was assessed by computing the differences in the orientation of the axes and location of the origins of each individual coordinate system from the average axes and the average origin, as described in Section 2.4. The mean differences, along with 95% confidence intervals, are presented here.

3. Results

3.1. Sensitivity analysis

The area of the articular facets selected by the two different protocols differed by a mean of 15% in the trapezium and by a mean of 18% in the metacarpal (Table 1). The mean differences between the orientations of the axes generated with the different facets were $0.7 \pm 0.7^{\circ}$, and the mean difference in the locations of the origins was 0.2 ± 0.1 mm (Table 1).

Table 1
The articular surface areas on the trapezium and the first metacarpal were manually selected optimally (P_1) and with a modified perimeter (P_2) to evaluate the sensitivity of the SCS coordinate systems to articular surface selection. Mean orientation and location differences between the coordinate systems generated with these two methods, along with standard variations, are presented in this table.

	Surface area (mm^2)		Orientation differences (deg.)			Location difference (mm)
	P_1	P_2	ΔX	ΔY	ΔZ	d(O)
TPM	140 ± 13	119 ± 13	0.6 ± 0.4	0.7 ± 0.5	1.3 ± 1.0	0.2 ± 0.1
MC1	153 ± 17	126 ± 14	0.7 ± 0.6	0.3 ± 0.4	0.3 ± 0.5	0.1 ± 0.1

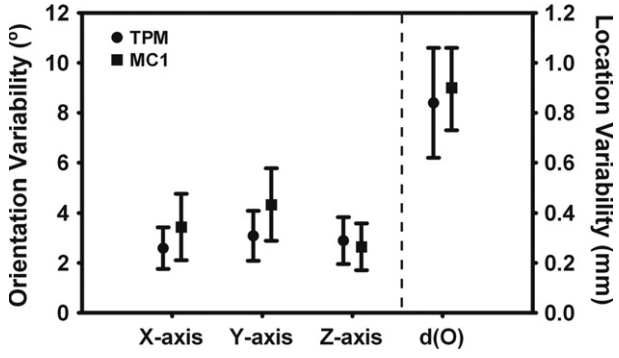

Fig. 5. Inter-subject variability in the trapezial (TPM) and the metacarpal (MC1) coordinate systems: the mean (along with the 95% CI) difference from the orientation of the average coordinate system in the x, y and z directions and the mean (along with the 95% CI) difference from the location of the average coordinate system.

3.2. Inter-subject variability

Overall, the orientation and the location of the trapezial coordinate system were slightly more consistent among subjects than those of the metacarpal coordinate system. The mean variation in the orientation of the TPM SCS axes was $2.8 \pm 2.3^{\circ}$, while the mean variation in the orientation of the MC1 SCS was $3.5 \pm 3.1^{\circ}$. The mean difference in the location of the TPM SCS was 0.8 ± 0.6 mm, whereas the mean difference in the location of the MC1 SCS was 0.9 ± 0.4 mm (Fig. 5).

4. Discussion

This communication describes a semi-automated method of generating the thumb CMC joint coordinate system (JCS) that aims to reduce kinematic cross-talk in data reporting. Our method builds on a prior adaptation of the ISB-recommended JSC that defines the internal/external rotation axis as the floating axis and flexion/extension and adduction/abduction as the body-fixed axes (Cheze et al., 2009). Its novelty lies in the computational alignment of the body-fixed axes with the principal directions of curvature in the joint, which are consistent features of the CMC joint that highly dictate motion.

Implementation of the coordinate system in joints from 24 healthy volunteers showed that the method presented here is insensitive to joint surface selection and that it is consistent across subjects. The bone models used for validation were extracted from CT volume images that were acquired with a resolution of $0.4 \times 0.4 \times 0.625$ mm, but the technique can also be applied to data acquired with lower resolution. The orientation of the axes should change only minimally with changes in image resolution, because the principal directions of curvature are computed from a polynomial surface that is fit to the data. This method may yield less satisfactory results in joints where the surface geometry is significantly distorted by trauma or degenerative conditions. At this point, however, it is also not clear what effect arthritis has on the shape of the joint features.

A potential criticism of our method may be the fact that internal/external rotation is expressed in terms of the floating axis, rather than a body-fixed axis that is aligned with the long axis of the metacarpal. Clinical descriptions of distal bone motion classically report axial rotation as rotation about the longitudinal axis of the distal bone. The use of a floating axis, however, is inherent to all Euler-based and ISB-recommended coordinate systems (Wu et al., 2005). Kinematic cross-talk is reduced when the axes of a JCS align as closely as possible with the axes of physiological motion. At the CMC joint, the primary axes of rotation are flexion/extension, embedded in the trapezium, and adduction/abduction, embedded in the metacarpal (Hollister et al., 1992; Imaeda et al., 1994). The assignment of internal/external rotation as the floating axis in the CMC JCS stems from these kinematic studies, and furthermore this choice has been supported theoretically and experimentally (Cheze et al., 2009). Ultimately, the method proposed here should reduce cross-talk and provide a robust approach for reporting the *in vivo* kinematics of the CMC joint.

Conflicts of interest statement

The authors have no financial or personal relationships that could bias this work.

Acknowledgments

The project described was supported by Grant number AR059185 from NIAMS/NIH and the American Foundation for Surgery of the Hand (AFSH). Its contents are the responsibility of the authors and do not necessarily represent the official views of the NIAMS or NIH. The authors would like to thank Joel B. Schwartz for his help with CT data acquisition and illustrations.

References

Cheze, L., Dumas, R., Comtet, J.J., Rumelhart, C., Fayet, M., 2009. A joint coordinate system proposal for the study of the trapeziometacarpal joint kinematics. Computer Methods in Biomechanics and Biomedical Engineering 12, 277–282.

Chèze, L., Dumas, R., Comtet, J.-J., Rumelhart, C., Fayet, M., 2012. Determination of the number of degrees of freedom of the trapeziometacarpal joint–an in vitro study. IRBM 33, 272–277.

Cooney, W.P., Lucca, M.J., Chao, E.Y., Linscheid, R.L., 1981. The kinesiology of the thumb trapeziometacarpal joint. Journal of Bone and Joint Surgery 63, 1371–1381.

Della Croce, U., Leardini, A., Chiari, L., Cappozzo, A., 2005. Human movement analysis using stereophotogrammetry. Part 4: assessment of anatomical landmark misplacement and its effects on joint kinematics. Gait Posture 21, 226–237.

Grood, E.S., Suntay, W.J., 1983. A joint coordinate system for the clinical description of three-dimensional motions: application to the knee. Journal of Biomechanical Engineering 105, 136–144.

Hollister, A., Buford, W.L., Myers, L.M., Giurintano, D.J., Novick, A., 1992. The axes of rotation of the thumb carpometacarpal joint. Journal of Orthopaedic Research 10, 454–460.

Imaeda, T., Niebur, G., Cooney, W.P., Linscheid, R.L., An, K.N., 1994. Kinematics of the normal trapeziometacarpal joint. Journal of Orthopaedic Research 12, 197–204.

Pieron, A.P., 1973. The mechanism of the first carpometacarpal (CMC) joint. An anatomical and mechanical analysis. Acta Orthopedica Scandinavica Supplementum 148, 1–104.

Wu, G., Cavanagh, P.R., 1995. ISB recommendations for standardization in the reporting of kinematic data. Journal of Biomechanics 28, 1257–1261.

Wu, G., Van der Helm, F.C., Veeger, H.E., Makhsous, M., Van Roy, P., Anglin, C., Nagels, J., Karduna, A.R., McQuade, K., Wang, X., Werner, F.W., Buchholz, B., 2005. ISB recommendation on definitions of joint coordinate systems of various joints for the reporting of human joint motion—Part II: shoulder, elbow, wrist and hand. Journal of Biomechanics 38, 981–992.